Calibration of PCB-132 Sensors in a Shock Tube

Dennis C. Berridge
NASA Langley Research Center, Hampton, VA 23681
School of Aeronautics and Astronautics, Purdue University, West Lafayette, IN 47907-1282

Steven P. Schneider
School of Aeronautics and Astronautics, Purdue University, West Lafayette, IN 47907-1282

ABSTRACT

While PCB-132 sensors have proven useful for measuring second-mode instability waves in many hypersonic wind tunnels, they are currently limited by their calibration. Until now, the factory calibration has been all that was available, which is a single-point calibration at an amplitude three orders of magnitude higher than a second-mode wave. In addition, little information has been available about the frequency response or spatial resolution of the sensors, which is important for measuring high-frequency instability waves. These shortcomings make it difficult to compare measurements at different conditions and between different sensors. If accurate quantitative measurements could be performed, comparisons of the growth and breakdown of instability waves could be made in different facilities, possibly leading to a method of predicting the amplitude at which the waves break down into turbulence, improving transition prediction.

A method for calibrating the sensors is proposed using a newly-built shock tube at Purdue University. This shock tube, essentially a half-scale version of the 6-Inch shock tube at the Graduate Aerospace Laboratories at Caltech, has been designed to attain a moderate vacuum in the driven section. Low driven pressures should allow the creation of very weak, yet still relatively thin shock waves. It is expected that static pressure rises within the range of second-mode amplitudes should be possible. The shock tube has been designed to create clean, planar shock waves with a laminar boundary layer to allow for accurate calibrations. Stronger shock waves can be used to identify the frequency response of the sensors out to hundreds of kilohertz.

1.0 INTRODUCTION

Measurements of boundary-layer instabilities in hypersonic tunnels are needed in order to improve methods for predicting transition in flight. Simple empirical correlations, such as Re_θ/M_e (Reynolds number based on momentum thickness divided by the edge Mach number) do not account for the mechanisms of transition, making it difficult to extrapolate results from each partial ground simulation to flight. Gathering enough data to establish a new correlation or the limits of an existing one can be prohibitively expensive, making a more analytical approach desirable.

Semi-empirical methods, such as e^N, use the growth of instabilities to predict transition location. Instability growth is computed as a ratio, $A/A_0 = e^N$, where A is the amplitude at a given location, and A_0 is the amplitude at the location at which the instability first starts to amplify. Transition is then empirically correlated to a certain

N factor. However, much is still uncertain when using e^N to predict transition. The initial amplitude of the instabilities is not accounted for, nor is it known at what amplitude the instabilities will break down.

Tunnel noise has been shown to have an impact on transition location, as well as the N factors at which transition occurs [1]. In flight, as well as in quiet tunnels, transition onset seems to occur at N factors between 8 and 11 [2, 3]. In conventional tunnels, transition onset usually occurs at N factors around 5 [4]. Pate also showed that transition on sharp cones at zero angle of attack can be correlated to measurements of tunnel noise [5]. While this correlation works well across a wide range of tunnels, the physical reasons behind it are poorly understood and it is unclear how it would apply to more complicated geometries.

It may be that increased noise levels lead to higher initial amplitudes of the second-mode waves, so that the waves require less amplification to break down. Another possibility is that increased noise levels feed into the nonlinear breakdown mechanisms, causing them to amplify sooner, leading to wave breakdown at a lower amplitude. Measurements of the growth and breakdown of second-mode waves, as well as freestream noise levels, are necessary to identify which mechanisms are actually important.

Understanding the effect of noise levels found in conventional tunnels on transition is necessary because no ground test facility is capable of fully reproducing flight conditions. While quiet tunnels can more accurately simulate flight noise levels, they are incapable of high Reynolds numbers, high Mach numbers, and high enthalpies. Since no single tunnel is able to simulate all aspects of flight, transition measurements must be made in multiple wind tunnels. If the effect of tunnel noise on transition can be understood, and measurements of boundary-layer instabilities can be made in the tunnels in which vehicles undergo testing, methods for extrapolating transition location from ground test to flight can further incorporate the physics of transition, improving accuracy and reducing risk. This is particularly critical since hypersonic flight tests are about a hundred times more expensive than ground tests, and generally return less data.

Measurements of tunnel noise and boundary-layer instabilities have been uncommon in hypersonic tunnels, mostly due to the difficulty of performing such measurements. Boundary-layer instabilities on models in hypersonic tunnels consist of low-amplitude, high-frequency fluctuations. Few instruments that are sensitive enough to measure the instabilities are also robust enough to survive inside a hypersonic wind tunnel. Hot wires have been the usual method of measurement in the past [6–8], but there are several disadvantages to the use of these sensors. While hot wires are capable of surviving in some hypersonic wind tunnels, their strength is marginal and they are prone to breaking. In many of the larger production tunnels where flight vehicles are tested, the conditions are too harsh for hot wires to survive at all.

Additionally, hot wires are an intrusive measurement technique, due to the shock wave and wake created by the probe. This means that only one point along a streamline can be measured at a time. Measurements at multiple points require multiple runs, or a longer run time combined with the ability to traverse the probe along the streamline. In facilities with short run times, requiring multiple runs at the same condition can result in unacceptably high costs.

The finding that some high-frequency pressure transducers can be used to measure second-mode waves is, therefore, of clear interest [9]. Second-mode waves, identified by Mack [10], are the dominant instability on flat plates and cones at zero angle of attack for Mach numbers above about 5. They can also be important for cones at low angle of attack and nearly 2D or axisymmetric geometries, such as scramjet forebodies or re-entry vehicles. Second-mode waves can be observed as high-frequency fluctuations in pressure, momentum flux, or heat transfer. The fact that they are a relatively easy-to-measure instability of engineering interest that can be isolated in a simple, well-understood flow makes them a good candidate for an investigation of noise effects and breakdown behavior under different conditions.

Pressure transducers can be mounted flush with a model's surface, so that multiple sensors can be placed along a single streamline, reducing the number of runs required to measure the development of the instabili-

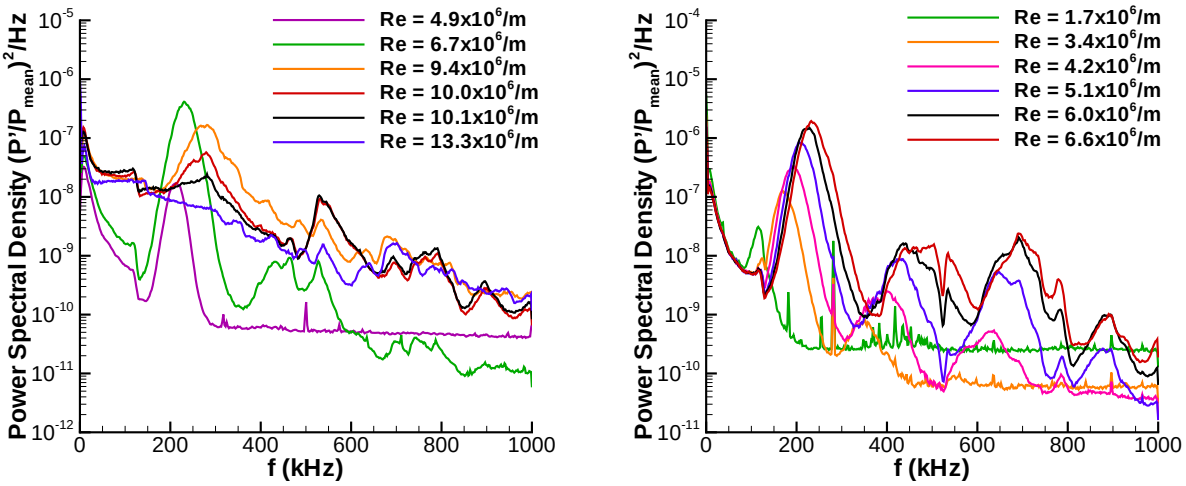

(a) Langley 15-Inch Mach 6 High-Temperature Tunnel

(b) Langley 31-Inch Mach 10 Tunnel

Figure 1: Measurements of second-mode waves using PCB-132 sensors

ties. The PCB-132 model of pressure transducer (see Ref. [11]) has also proven to be quite robust, capable of surviving in many hypersonic tunnels, with a low incidence of broken sensors [12–17]. These qualities make attempting instability measurements feasible, even in many of the large tunnels used to test vehicles. Samples of wind tunnel data obtained with these sensors are shown in Figure 1 (from Ref. [18]), which shows measurements on a 7° half-angle cone in the NASA Langley 15-Inch Mach 6 High-Temperature and 31-Inch Mach 10 tunnels.

The second-mode waves are evident from the large, broad peaks in the power spectra. Waves can be observed to grow, become nonlinear (shown by the appearance of multiple peaks, which are harmonics) and break down into turbulence. A turbulent spectrum is one with high levels of fluctuations at all frequencies, with no particular peak and fluctuation strengths that generally decrease with increasing frequency. Information about the growth and stage (linear growth, nonlinear growth, breakdown, or turbulence) of the instabilities can be useful for interpreting changes in transition location measured through other means, such as temperature or heat flux measurements.

Measurements performed with PCBs at similar conditions in multiple tunnels have shown possible differences in wave amplitude. An example is shown in Figure 2. Measurements on the same 7°-degree half-angle cone model in the Langley 15-Inch Mach 6 High-Temperature Tunnel, the Langley 20-Inch Mach 6 Tunnel, and the Boeing/AFOSR Mach 6 Quiet Tunnel (BAM6QT) at Purdue are shown. The measurements at Purdue were performed under noisy flow conditions, under which the Purdue tunnel is expected to have higher freestream noise levels than the Langley tunnels. Measurements from Purdue are shown at two different unit Reynolds numbers, one higher and one lower than the condition in the Langley tunnels, since a matching condition was not available. The frequencies of the waves in the Purdue tunnel are slightly lower than those in the Langley tunnels for an unknown reason. The waves clearly appear much larger in the Purdue tunnels than in the Langley tunnels at both conditions, indicating that some tunnel characteristic, most likely the freestream noise levels, is influencing the wave amplitude. A significant difference in amplitude is observed between the two Langley tunnels, as well, with larger waves in the 15-Inch High-Temperature tunnel. This is the expected result, since

a smaller tunnel would be expected to have higher freestream noise levels. These types of measurements have shown that PCB-132 sensors can potentially be very useful in examining hypersonic boundary-layer instabilities.

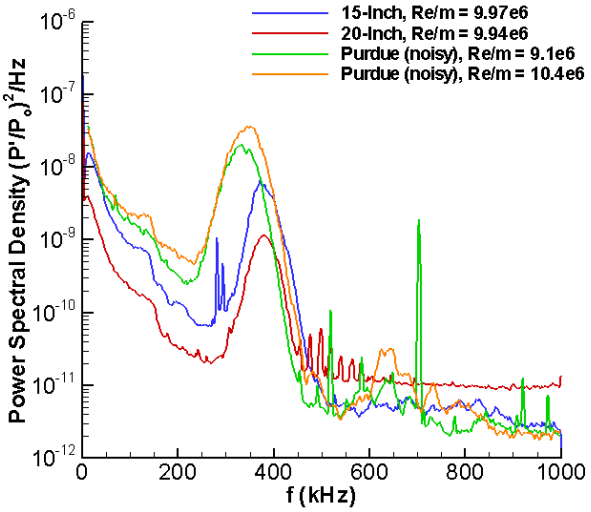

Figure 2: PCB measurements in the BAM6QT, 15-Inch Mach 6 High-Temperature Tunnel, and 20-Inch Mach 6 Tunnel. 7° cone model, $x = 0.208$ m.

2.0 INSTRUMENTATION

PCB-132 sensors are piezoelectric pressure transducers designed to measure the time of arrival of shock waves. They are high-pass filtered at 11 kHz, with a quoted resonant frequency above 1 MHz. The manufacturer calibrates the sensors in a shock tube, by running one shock with a strength close to 7 kPa past the sensor. The calibration is assumed to be linear, with a 0 V offset.

The manufacturer's calibration is not necessarily relevant or sufficiently accurate for the purposes of instability measurements. The response for an input of 7 kPa is not necessarily similar to the response for an instability wave, which has pressure fluctuations three orders of magnitude smaller. In addition, the frequency response for the sensor is not identified. Second-mode instabilities in wind tunnels typically have frequencies between 100 and 600 kHz, so the frequency response of the sensor may be important to determining the actual magnitude of the pressure fluctuations across this frequency range.

Another issue with PCB-132 sensors is their spatial resolution. The instability waves on models generally have wavelengths on the order of millimeters. The sensing surface on the PCB sensors is 0.125 inches, or about 3.2 mm, which is often longer than the second-mode wavelength. However, the sensing element is only a 0.03 x 0.03-in square (0.762 x 0.762 mm). The sensing element is visible as a brown square in Figure 3. While this is smaller, the size may still be significant when compared to the second-mode wavelength. If the sensor size is significant compared to the wavelength, there will be spatial averaging. This averaging must be taken into account to find accurate amplitudes, so it is necessary to know over what area the sensor is measuring.

While the sizes of the sensing surface and sensing element are known, the area over which the sensor actually senses pressure (the active sensing area), is unknown. This is because the sensing surface and sensing

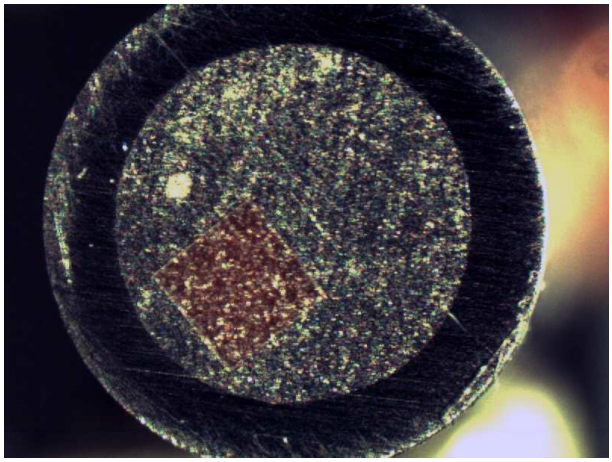

Figure 3: PCB-132 sensor with epoxy removed, showing the sensing element (brown square).

element are both covered with a conductive epoxy. Pressure is transmitted to the sensing element through the epoxy, but the manner in which this happens is not well-defined. The sensing area may depend on the magnitude of the pressure fluctuation, as well as the actual thickness of the layer, which may vary between sensors. This makes it necessary to determine the sensing area of the sensors while calibrating them. As indicated in Figure 3, the sensing element is not precisely located on the sensor. The effective sensing area may depend on the location and orientation of the sensing element. These will need to be determined without removing the epoxy layer.

3.0 METHOD OF CALIBRATION

The most obvious method to calibrate the sensors is to create pressure fluctuations at fixed frequencies and known magnitudes and measure the sensor response. However, creating controlled fluctuations at the high frequencies required is very difficult. Ultrasonic emitters cannot readily reach the high end of the PCB frequency range, and accurate reference sensors to confirm the magnitude of the pressure fluctuations are difficult to find at these high frequencies.

An alternative is to use a step input or impulse as the calibration input. In theory, these inputs excite all response frequencies, enabling the entire frequency response to be identified using a single input. The high-frequency content is small so that averaging multiple step responses is likely required to obtain good high-frequency signal.

For a pressure transducer, a step input can be approximated with a shock wave. These can be generated using a shock tube or a laser perturber, but the flow in a shock tube is better understood. For this reason, it was decided to attempt to calibrate the PCB sensors using a shock tube. In order to calibrate for instability measurements, very weak, thin shock waves must be created. Thin shock waves are required to approximate the step input. Since a shock has some finite thickness, it is not really a step input, but if the shock passes over the sensor in a time sufficiently small compared to the response time of the sensor, it will closely approximate a step input. The rise time of PCB-132 sensors depends on the input voltage, varying from 65 to 312 nanoseconds for output voltages between 1 V and 5 V (about 70 kPA and 340 kPa, respectively).

3.1 Shock Strength and Passage Time

Unfortunately, a small shock passage time and a weak shock are competing goals, since a shock becomes thicker and moves more slowly as it becomes weaker. This can be mitigated somewhat by using a low driven pressure in the shock tube, since the strength of the shock depends on the pressure ratio across the shock, and not the actual pressures. With a low driven pressure, the pressure ratio can be large even if the pressure difference across the shock is small. This can only work to a point, since eventually the driven section becomes rarefied and the shock begins to thicken again as the mean free path increases.

The point at which the shock becomes too thick to provide a useful calibration input is unclear, but some simple methods have been used to estimate it. The shock thickness was calculated using Taylor's solution for the thickness of weak shocks [19]. The time for the shock to pass was found using the standard shock tube equations for shock speed. The pressure across the shock (diaphragm burst pressure) was kept constant at 7 kPa, and the driven pressure was varied. The results from this analysis are shown in Figure 4.

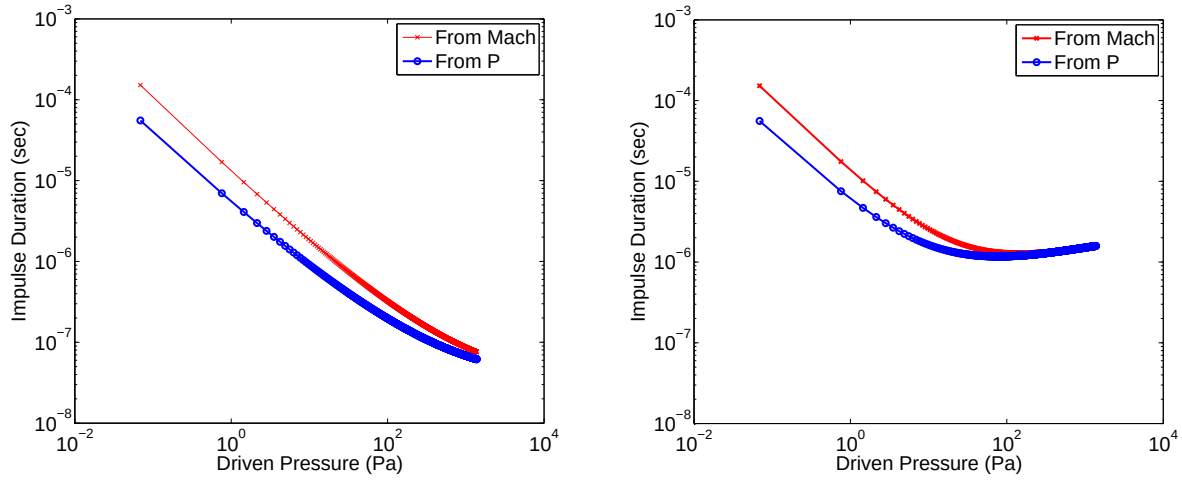

(a) Pitot configuration

(b) Static configuration

Figure 4: Calculated impulse duration (shock passage time) for shocks made with a 7 kPa burst pressure differential and varying driven pressures.

As illustrated in Figure 4, the time for the shock to pass over the sensor depends heavily on the orientation of the sensor. Two lines are shown, since the shock thickness can be calculated from the Mach number and the pressure difference. The two answers do not always agree, for some unknown reason, so both results are shown. If the sensor is mounted perpendicular to the flow (here called pitot configuration because the sensor measures the pitot pressure), the minimum time for the shock to pass over the sensor in the cases shown is about 100 nanoseconds, though it is clear that smaller impulse times are achievable if the driven pressure is increased. If the sensor is mounted parallel to the flow (here called static configuration because the sensor measures the static pressure), the minimum time for the shock to pass is about 1 μs, an order of magnitude larger. The difference is caused by the fact that in static configuration, the whole shock must pass over the whole sensing area before the impulse is complete, whereas in pitot configuration, the shock only needs to pass completely through the plane of the sensing surface. This means that in static configuration, the shock needs to travel a distance equal to the thickness of the shock plus the length of the active sensing area to complete the impulse, but in pitot configuration it needs only travel a distance equal to the thickness of the shock. In most cases, the

shock is very thin compared to the length of the sensing area, so the impulse duration is much larger in static configuration than in pitot configuration.

The pitot pressure step is larger than the static pressure step, so again it becomes difficult to have both a small pressure rise and a short impulse duration. It may be necessary to identify the frequency response in pitot configuration using shocks too strong to be relevant to instability measurements, and then find the calibration curve of the sensors using shocks too thick to identify the frequency response. Assuming that the frequency response does not depend much on the magnitude of the input, this method should yield good calibrations. Calibration curves will be obtained in both configurations to see if the configuration affects the linearity or slope of the curve. Using thick shocks with sensors in pitot configuration should show how much the impulse duration affects the calibration.

3.2 Burst Diaphragms

Creating very weak shocks with static pressure rises comparable to second-mode amplitudes in wind tunnels presents another challenge. Achieving low pressure rises is made easier with a low burst pressure differential. This is because increasing the Mach number of the shock decreases the pressure rise for a given burst differential. For high burst differentials, the driven pressure must be reduced to a very low vacuum, at which point the shock has become too thick to be useful. For a small burst differential, however, a higher driven pressure may be used, and it is possible to adjust the driven pressure to give a thinner shock of the desired strength.

While a lower burst differential is desirable, it is difficult to create in practice. A material is required that is very weak so that it breaks at a low pressure difference, but also strong enough to withstand installation in the shock tube, and not too porous so that air does not leak through it and make maintaining a low driven pressure difficult. Previous work at Purdue indicated that small burst pressures on the order of 1 PSI (7kPa) are possible [20]. These low burst pressures have not yet been replicated during this effort. Work is continuing to recover this capability.

If a material cannot be found that naturally bursts at a low pressure differential, methods may be used to force a stronger material to burst at these pressures. The likely method for this shock tube is an electrical system similar to what was used on the Mach 4 Quiet Ludweig Tube at Purdue [21]. In this type of system, wires are taped to the diaphragm face and attached to a system that can generate a large current for a short time. The current causes the wires to heat up, weakening the diaphragm material and causing it to burst. Since this shock tube will be using small, thin diaphragms, the power required for this system should not be very high. Other methods of lowering the burst pressure of a diaphragm may also be tried, including scoring by hand and folding the diaphragm.

3.3 Identifying Active Sensing Area

It may be possible to identify the length of the active sensing area by testing the sensors in static configuration. If the shock passes over the sensor slowly enough that the response time of the sensor is insignificant, the rise time will show how long it took the shock to pass over the active sensing area. This is because the shock activates the sensing area slowly as it passes over the area. If the thickness and speed of the shock are known, the length of the sensing area can be calculated from the rise time. Different shock strengths can be used to see if the size of the active area is dependent on the magnitude of the input.

4.0 EXISTING SHOCK TUBE MEASUREMENTS

Some experiments were performed in the existing shock tube at Purdue located in Armstrong Hall. This shock tube has an internal diameter of 10.8 cm, a 0.64 m driver section, and a 4.67 m driven section. Weak shocks could not be created in this shock tube because of the poor vacuum performance of the tube, which prevented reaching low driven pressures. However, the sensors could be calibrated over a reasonable range of pressures when mounted in static configuration.

The pressure rise across the shock was calculated from the ideal shock equations based on the speed of the shock and measured by the reference pressure sensors (Kistler 603B1 piezoelectric transducers). The speed of the shock was calculated from the arrival times at two different sensor locations. The measurements do not agree with the calculations, and it is unclear which is more accurate. Both are shown in Figure 5.

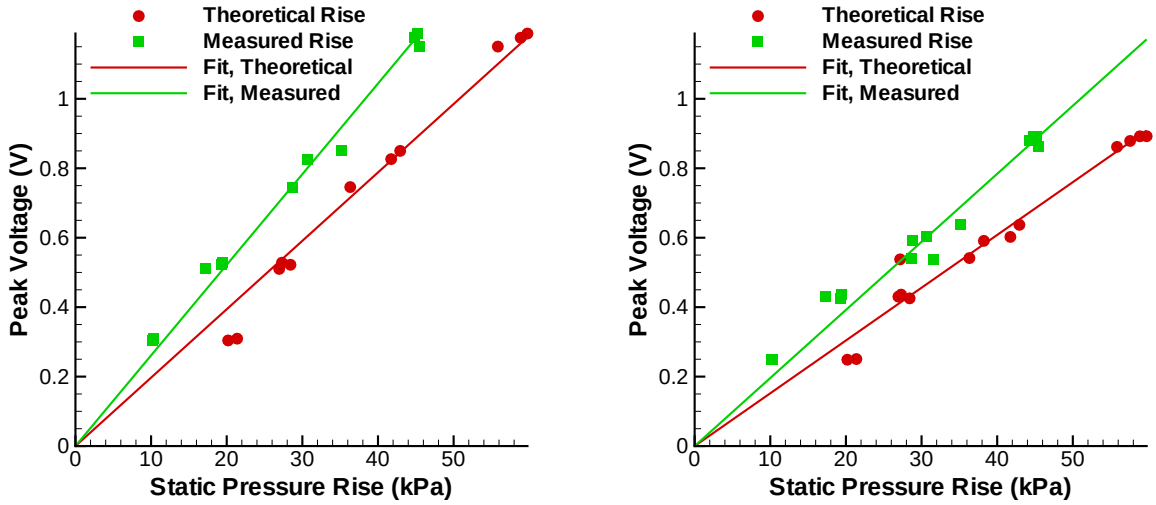

(a) Calibration for PCB #5045

(b) Calibration for PCB #5194

Figure 5: Calibration curves for two PCB-132A31 sensors.

It is clear in Figure 5 that the calibrations are linear over the measured range for both sensors. The manufacturer's calibration falls between the the two calibrations found for each sensor, indicating that for this range of pressures, the manufacturer's calibration gives at least a good estimate of the pressure measured by the sensor.

The sensor shock response was measured in both static and pitot configurations, as shown in Figure 6. The two responses are generally similar, showing a sharp rise when the shock passes, followed by a slower decline back to 0 V after about 0.1 ms. This is expected, since the sensors are high-pass filtered at 11 kHz. The decline takes slightly longer in static configuration, probably due to the longer impulse time. Note that in static configuration, the shock reaches the sensor at about 0.75 msec, not 0 msec. The major difference between the two is that a high-frequency oscillation is present in the pitot response. The frequency of this oscillation varies between sensors, and was observed to occur between 800 kHz and 1.2 MHz. The reason for the oscillation is uncertain, but it seems likely that it is caused by excitation of the resonant frequency of the sensor. The resonance may not be excited in static configuration due to the longer impulse duration. In addition, in pitot configuration, the response to a given pressure rise is amplified by more than 300% compared to the response in static configuration. This might indicate an overshoot caused by the resonance of the sensor.

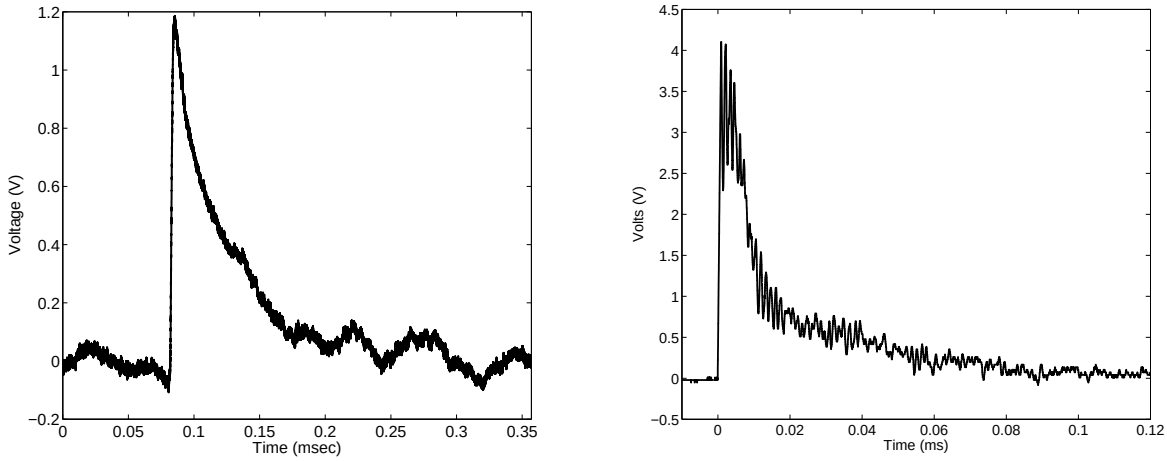

(a) Static configuration

(b) Pitot configuration

Figure 6: PCB shock responses.

Some attempts have been made to model the frequency response of the sensor using the tools provided with Matlab®. Some examples are shown in Figure 7. Models found using an output-error method have the prefix “OE” followed by three numbers. The first is the order of the numerator, the second is the order of the denominator, and the third is the delay of the signal. The delay was always specified to be zero. Process models begin with “P”, followed by the order of the numerator. If the model has a zero, the next letter is “Z”. If the model is second-order and underdamped, meaning that the poles are complex, a “U” is appended to the name. For example, a second-order underdamped process model with a zero would be called “P2ZU”. The model from PCB is a step response calculated from a transfer function found by taking the product of the transfer functions for a simple high-pass filter and a first-order system, which is what PCB stated was the system type for this sensor.

For the static-mounted case, many of the models do an acceptable job of following the roll-off (Fig. 7a), but they all do a poor job of following the rise (Fig. 7b). Since the rise is the most important part of the response, this shows that these models have not done well. In Figures 7c and 7d, the results are seen to be mixed. Most of the models completely fail to model the step response. However, Model OE240 follows the rise and the roll-off fairly well, although it fails to model the oscillations. This may be due to attempts by the modeling algorithm to prevent the model from following noise.

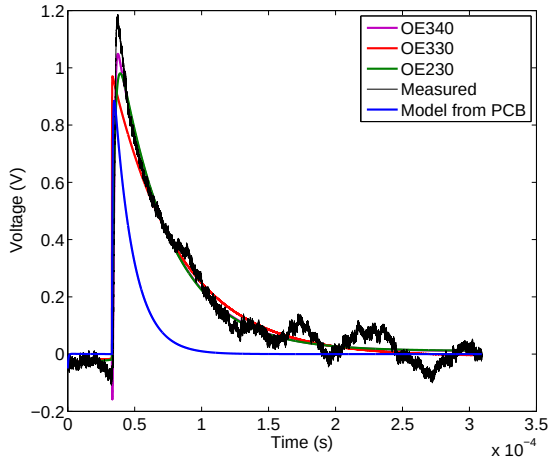

(a) Static-mounted case.

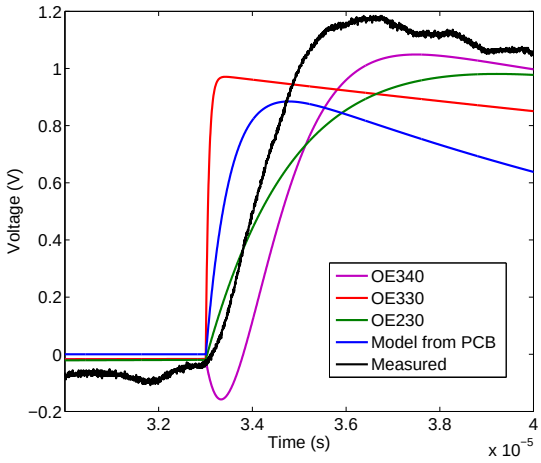

(b) Detail of rise times, static-mounted.

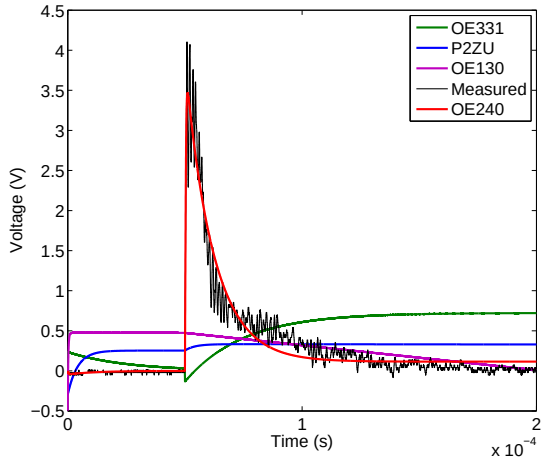

(c) Pitot-mounted case.

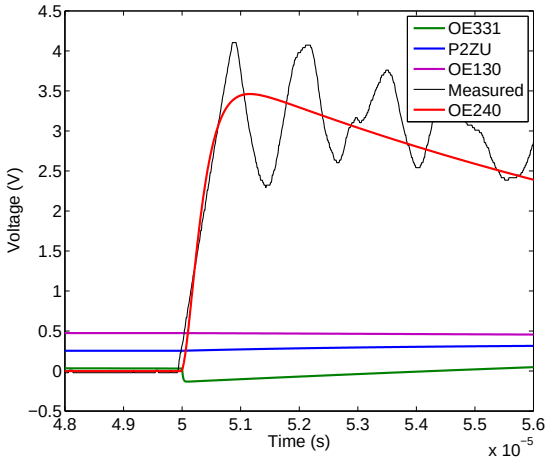

(d) Detail of rise times, pitot-mounted.

Figure 7: Measured and modeled time-domain responses for the static- and pitot-mounted cases.

While it is clear that the current attempts fail to adequately model the sensor, it seems that a modeling technique can be found. The responses used for fitting the model need to be improved. The current attempts were made on single responses, with no averaging, which gives a noisy signal and makes fitting a model more difficult. It may also be necessary to try to fit the models in the frequency domain instead of the time domain, to give more importance to the rise rather than the roll-off. Collaboration with others who are more experienced in system modelling would be helpful.

5.0 NEW SHOCK TUBE

In order to create the weak shocks required for calibration, a new shock tube has been built with a design based on the 6-inch shock tube in the Graduate Aerospace Laboratories at Caltech (GALCIT). The new shock tube (Figure 8) has a 3.5-inch (15.2-cm) inner diameter, a 12-foot (3.6-m) driven section, and a four-foot (1.2-m) driver section. PCB has expressed interest in the data that may be gathered from this shock tube, and will be cooperating with the development of the calibration techniques.

The performance of this shock tube is currently being characterized. The driven section should be able to reach pressures of 1 millitorr (100 Pa) using an Oerlikon TRIVAC D4B vacuum pump, and the driver section is designed to withstand pressures as high as 6895 kPa. The current maximum pressure will be 970 kPa, which is the supply pressure in the building. The interior of the tube was honed, and the joints of the shock tube have been designed to be smooth, so as to avoid disturbing the flow and create a clean planar shock wave with a following laminar boundary layer. A laser-differential interferometer (LDI) may be used as a reference sensor to measure the thickness of the shock waves that pass. This shock tube will enable the measurement of weak waves, to check the calibration of the sensors to low amplitudes. The current estimate of the smallest static pressure rise achievable in this shock tube is 7 Pa, which is within the upper range of second-mode amplitudes in wind tunnels. It should also be possible to perform repeated low-noise measurements, so that the frequency response of the sensors can be identified.

In order to use weak diaphragms at low driven pressures, it is necessary to reduce the driver section to pressures around 7 kPa. To allow for this, the driver section is connected to the vacuum system close to the end of the driven section. Cut-off valves allow the driven section to continue to be pumped down after the driver section has reached the appropriate pressure and protect the vacuum system from the high pressures that will sometimes be present in the driver section.

6.0 CONCLUSIONS

PCB-132 sensors show promise for improving the current understanding of noise effects on transition, and improving the state of the art for transition measurements in large hypersonic wind tunnels. Accurate calibrations would be useful for this effort. A small shock tube has been designed and built that should be able to provide reasonably accurate and useful calibrations for instability measurements. Calibrations will be performed using shock waves to approximate a step input to identify the frequency response of the sensors, and weak shocks with pressure rises comparable to second-mode wave amplitudes. An attempt at identifying the spatial resolution of the sensors by examining the rise times for shocks of known thickness will also be made. It is expected that the first calibrations of sensors using this shock tube will be made this year.

Figure 8: The new shock tube at Purdue.

ACKNOWLEDGMENTS

Jerry Hahn in the Purdue AAE department machine shop made the parts for the shock tube. Ana Kerlo, a graduate student at Purdue, also assisted with the design of the shock tube. Joe Jewell at Caltech sent drawings of the original shock tube. Jason Damazo, also at Caltech, provided information about the design and operation of the original shock tube. This work has been funded in part by AFOSR and the NASA Aeronautics Scholarship Program.

REFERENCES

[1] Beckwith, I. E. and Miller III, C. G., "Aerothermodynamics and Transition in High-Speed Wind Tunnels at NASA Langley," *Annual Review of Fluid Mechanics*, Vol. 22, 1991, pp. 419–439.

[2] Schneider, S. P., "Flight Data for Boundary-Layer Transition at Hypersonic and Supersonic Speeds," *Journal of Spacecraft and Rockets*, Vol. 36, No. 1, 1999, pp. 8–20.

[3] Chen, F.-J., Malik, M., and Beckwith, I., "Boundary-Layer Transition on a Cone and Flat Plate at Mach 3.5," *AIAA Journal*, Vol. 27 No. 6, June 1989, pp. 687–693.

[4] Alba, C., Johnson, H., Bartkowicz, M., Candler, G., and Berger, K., "Boundary Layer Stability Calculations for the HIFiRE-1 Transition Experiment," *Journal of Spacecraft and Rockets*, Vol. 45, No. 6, January 2008, pp. 1125–1133.

[5] Pate, S. R., "Measurements and Correlations of Transition Reynolds Numbers on Sharp Slender Cones at High Speeds," *AIAA Journal*, Vol. 9, No. 6, 1971, pp. 1082–1090.

[6] Stetson, K. F. and Kimmel, R. L., "On Hypersonic Boundary-Layer Stability," Paper 1992-0737, AIAA, January 1992.

[7] Demetriades, A., "An experiment on the stability of hypersonic laminar boundary layers," *Journal of Fluid Mechanics*, Vol. 7, No. 3, 1960, pp. 385–396.

[8] Kendall, J., "Wind Tunnel Experiments Relating to Supersonic and Hypersonic Boundary-Layer Transition," *AIAA Journal*, Vol. 13, No. 3, 1975, pp. 290–299.

[9] Fujii, K., "Experiment of Two Dimensional Roughness Effect on Hypersonic Boundary-Layer Transition," *Journal of Spacecraft and Rockets*, Vol. 43, No. 4, July-August 2006, pp. 731–738.

[10] Mack, L. M., "Linear Stability Theory and the Problem of Supersonic Boundary-Layer Transition," *AIAA Journal*, Vol. 13, No. 3, 1975, pp. 278–289.

[11] "PCB Piezotronics Model 132A31," http://pcb.com/spec_sheet.asp?model=132A31&item_id=5190.

[12] Estorf, M., Radespiel, R., Schneider, S. P., Johnson, H., and Hein, S., "Surface-Pressure Measurements of Second-Mode Instability in Quiet Hypersonic Flow," Paper 2008-1153, AIAA, January 2008.

[13] Casper, K. M., Beresh, S. J., Henfling, J. F., Spillers, R. W., Pruett, B., and Schneider, S. P., "Hypersonic Wind-Tunnel Measurements of Boundary-Layer Pressure Fluctuations," Paper 2009-4054, AIAA, June 2009, revised November 2009.

[14] Alba, C. R., Casper, K. M., Beresh, S. J., and Schneider, S. P., "Comparison of experimentally measured and computed second-mode disturbances in hypersonic boundary-layers," Paper 2010-897, AIAA, January 2010.

[15] Lukashevich, S., Maslov, A., Shiplyuk, A., Fedorov, A., and Soudakov, V., "Stabilization of high-speed bounday layer using porous coatings of various thicknesses," Paper 2010-4720, AIAA, June-July 2010.

[16] Bounitch, A., Lewis, D. R., and Lafferty, J. F., "Improved Measurements of "Tunnel Noise" Pressure Fluctuations in the AEDC Hypervelocity Wind Tunnel No. 9," Paper 2011-1200, AIAA, January 2011.

[17] Rufer, S. J. and Berridge, D. C., "Experimental Study of Second-Mode Instabilities on a 7-Degree Cone at Mach 6," Paper 2011-3877, AIAA, June 2011.

[18] Berridge, D. C., Casper, K. M., Rufer, S. J., Alba, C. R., Lewis, D. R., Beresh, S. J., and Schneider, S. P., "Measurements and Computations of Second-Mode Instability Waves in Several Hypersonic Wind Tunnels," Paper 2010-5002, AIAA, June 2010.

[19] Thompson, P. A., *Compressible-Fluid Dynamics*, McGraw-Hill, 1988.

[20] Rotea, M. A., Randall, L. A., Song, G., and Schneider, S. P., "Model Identification of a Kulite Pressure Transducer," Paper 96-2278, AIAA, June 1996.

[21] Schneider, S. P., Collicott, S. H., Schmisseur, J., Ladoon, D., Randall, L. A., Munro, S. E., and Salyer, T., "Laminar-Turbulent Transition Research in the Purdue Mach-4 Quiet-Flow Ludweig Tube," Paper 1996-2191, AIAA, June 1996.